Glenoid bony morphology of osteoarthritis prior to shoulder arthroplasty: what the surgeon wants to know and why

Lawrence Lo[1] · Scott Koenig[2] · Natalie L. Leong[2,3] · Brian B. Shiu[2] · S. Ashfaq Hasan[2,4] · Mohit N. Gilotra[2,5] · Kenneth C. Wang[1,6]

Abstract

Shoulder arthroplasty is performed with increasing frequency, and osteoarthritis is the most common indication for this procedure. However, the glenoid side of the joint is widely recognized as a limiting factor in the long-term durability of shoulder replacement, and osteoarthritis leads to characteristic bony changes at the glenoid which can exacerbate this challenge by reducing the already limited glenoid bone stock, by altering biomechanics, and by interfering with operative exposure. This article reviews the Walch classification system for glenoid morphology. Several typical findings of osteoarthritis at the glenoid are discussed including central bone loss, posterior bone loss, retroversion, biconcavity, inclination, osteophyte formation, subchondral bone quality, and bone density. The three primary types of shoulder arthroplasty are reviewed, along with several techniques for addressing glenoid deformity, including eccentric reaming, bone grafting, and the use of augmented glenoid components. Ultimately, a primary objective at shoulder arthroplasty is to correct glenoid deformity while preserving bone stock, which depends critically on characterizing the glenoid at pre-operative imaging. Understanding the surgical techniques and the implications of glenoid morphology on surgical decision-making enables the radiologist to provide the morphologic information needed by the surgeon.

Keywords Shoulder arthroplasty · Osteoarthritis · Glenoid · Component loosening · Surgical techniques

Introduction

The number of shoulder arthroplasties performed in the United States over the past decade has sharply increased with one nationwide study reporting a 24% increase from 2011–2014 alone [1]. Although there are many indications for shoulder replacement surgery, osteoarthritis is the most common [2]. The glenoid side of the joint is widely recognized as a limiting factor for the long-term durability of shoulder replacement, due to the risk of glenoid component malpositioning and early loosening [3–7]. Glenohumeral osteoarthritis is associated with several characteristic bony changes occurring at the glenoid which can exacerbate this challenge, by reducing the limited bone stock, by altering the biomechanics of glenohumeral articulation, and by interfering with operative exposure of the glenoid. Consequently, surgical planning depends critically on characterizing glenoid bony morphology at pre-operative imaging. This article reviews key morphologic changes of osteoarthritis at the glenoid, explains the critical role of glenoid bone stock in arthroplasty durability, and describes the range of surgical techniques used to manage glenoid deformity, in order to inform the image interpretation process.

✉ Kenneth C. Wang
   kcwang@gmail.com

1   Department of Diagnostic Radiology and Nuclear Medicine, University of Maryland, School of Medicine, 22 S. Greene St, Baltimore, MD 21201, USA

2   Department of Orthopaedics, University of Maryland, School of Medicine, 22 S. Greene St, Baltimore, MD 21201, USA

3   Department of Orthopaedics, University of Maryland, School of Medicine, 110 S. Paca Street, 6th Floor, Baltimore, MD 21201, USA

4   Department of Orthopaedics, University of Maryland, School of Medicine, 2200 Kernan Drive, Suite 1154, Baltimore, MD 21207, USA

5   Department of Orthopaedics, University of Maryland, School of Medicine, 100 Penn Street, Room 540D, Baltimore, MD 21201, USA

6   Imaging Service, Baltimore VA Medical Center, 10 N. Greene St, Rm. C1-24, Baltimore, MD 21201, USA

Types of shoulder arthroplasty

Anatomic total shoulder arthroplasty (TSA) is the most common type of shoulder arthroplasty performed for osteoarthritis [1]. Most anatomic TSA glenoid components in use today are composed entirely of polyethylene, except for a radiopaque marker which is often present (Fig. 1a). Glenoid component loosening is widely recognized as a primary limiting factor in the long-term durability of anatomic TSA. A variety of glenoid component designs have been introduced to minimize loosening. Components with threaded pegs (i.e., pegged components) have demonstrated a lower rate of radiographic loosening (as evidenced by periprosthetic lucency) when compared to keeled components, which instead have a central wedge attached to the articulating polyethylene liner [3]. Of note, metal-backed glenoid components have been shown to contribute to higher revision rates for reasons other than loosening, such as screw breakage and component separation due to accelerated wear of the polyethylene portion [8].

Reverse TSA has grown rapidly in popularity over the past decade. The original indication was for rotator cuff tear arthropathy involving a massive irreparable cuff tear with glenohumeral arthritis. As experience with reverse TSA has grown and the complication rate has decreased, these indications have gradually expanded to now include: older patients with massive irreparable rotator cuff tears even in the absence of arthritis, reconstruction after tumor resection, acute proximal humerus fractures, and osteoarthritis with an intact rotator cuff but significant glenoid bone loss. The glenoid portion of reverse TSA consists of two parts. The metaglene, or baseplate, is affixed to the native glenoid by threaded screws and a long central peg or screw, and the glenosphere (attached to the metaglene) provides the convex articulating surface (Fig. 1b).

Hemiarthroplasty (HA) is the least commonly performed shoulder arthroplasty for glenohumeral osteoarthritis and does not utilize a glenoid component (Fig. 1c). In HA, a humeral component resurfaces or replaces the humeral head, and articulates directly with the native glenoid. By avoiding the use of a glenoid component, HA does not suffer from glenoid component loosening. However, glenoid derangements of osteoarthritis are not corrected in HA, thus preventing the restoration of normal biomechanics or relief of pain generated from the glenoid side. While a further refinement (i.e., HA with non-prosthetic glenoid arthroplasty, also referred to as the "ream-and-run" variant of HA) has been used, this procedure may require prolonged post-operative rehabilitation. There is also a risk of progressive erosive bone loss of the glenoid from the metal-on-bone articulation. Ultimately, in osteoarthritis, HA is associated with less pain relief, poorer functional outcome, and higher rates of revision surgery when compared to total shoulder arthroplasty [9, 10]. However, in the setting of cuff tear arthropathy (CTA), if a patient is deemed not to be a candidate for reverse TSA, CTA hemiarthroplasty may be an option. This utilizes a specialized humeral component which has a larger articular surface than the anatomic humeral head, to allow for articulation with both the glenoid and acromion.

Glenoid component failure

Loosening of the glenoid component is the primary mode of glenoid component failure for anatomic TSA [6, 7]. The mechanism for glenoid component loosening is classically
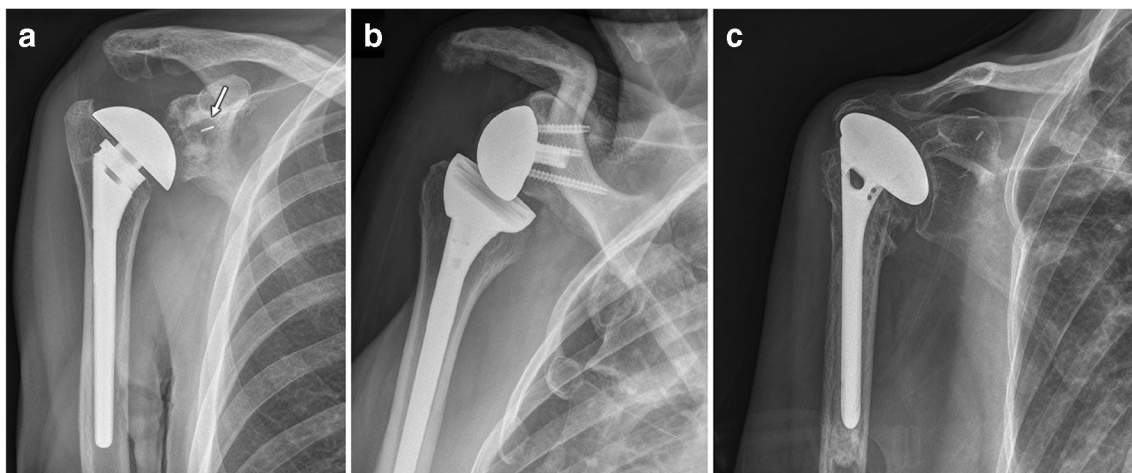

Fig. 1 Types of shoulder arthroplasties. **a** 58-year-old man with anatomic total shoulder arthroplasty. Anteroposterior radiograph of the right shoulder demonstrates the metallic humeral component with stem, and the polyethylene glenoid component with a small linear radiopaque marker (arrow) at the central peg. **b** 65-year-old man with reverse total shoulder arthroplasty. Oblique frontal radiograph of the right shoulder shows the metallic stem and cup of the humeral component, and the metallic glenoid component. The latter consists of the convex articulating portion (glenosphere), attached to a baseplate-screw construct (metaglene). **c** 66-year-old female with shoulder hemiarthroplasty. Anteroposterior radiograph of the right shoulder shows the cemented metallic humeral component articulating with the native glenoid

Fig. 2 A 72-year-old woman with anatomic total arthroplasty complicated by glenoid component loosening. Frontal radiograph of the right shoulder shows extensive periprosthetic lucencies and cystic changes surrounding the polyethylene pegs of the glenoid component. At the time of surgery, the glenoid component was found to be grossly loose and was removed

explained by the "rocking horse phenomenon" [3], which involves edge loading causing progressive breakdown from micromotion at the bone-implant interface over time (Fig. 2). The Lazarus classification has been frequently cited for the grading of all-polyethylene glenoid component loosening [11]. Indirect signs of loosening include changes in component positioning or progressive periprosthetic lucency on sequential radiographs [12].

Glenoid loosening in reverse TSA, while rare when compared to anatomic TSA, typically occurs at the baseplate due to component malpositioning in the absence of infection [4, 5]. Longitudinal studies by Melis et al. suggested that loosening is present when radiolucent lines of > 2 mm completely surround either the glenoid screws, the central peg, or the baseplate-bone interface [13, 14]. As a closely related entity, scapular notching is a common complication of reverse TSA which can lead to glenoid component loosening. A common grading scheme for scapular notching was described by Siveaux et al. [15]: Grade 1 for notching limited to the scapular pillar, Grade 2 for notching reaching the inferior screw, Grade 3 for notching extending over the inferior screw, and Grade 4 for notching extending under the baseplate. Similar to anatomic TSA, glenoid component loosening in reverse TSA can lead to instability, functional decline, and eventual arthroplasty failure (Fig. 3).

Glenoid morphology in glenohumeral osteoarthritis

While many types of glenohumeral derangement may lead to a need for arthroplasty, osteoarthritis is the most common
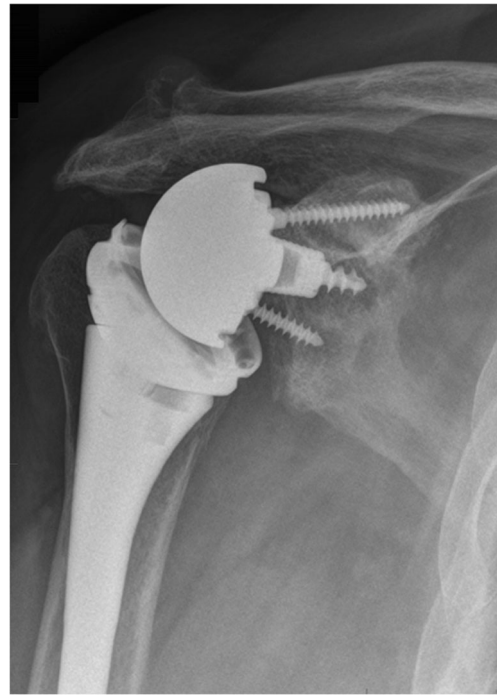

Fig. 3 A 69-year-old man with reverse total shoulder arthroplasty complicated by loosening of the glenoid component. Frontal radiograph shows radiolucent lines surrounding the central peg and the glenoid screws with distraction of the metaglene from the glenoid, consistent with glenoid component loosening

indication for total shoulder replacement. Glenohumeral osteoarthritis causes several characteristic bony changes at the glenoid. The Walch classification system for characterizing glenoid morphology in osteoarthritis was first described in 1993 [16], with subsequent modification in 2016 [17].

This modified Walch classification is summarized in Table 1 and illustrated in Fig. 4. Type A glenoids demonstrate concentric wear without humeral head subluxation. This wear may be minor (type A1) or major (type A2). Type B glenoids are characterized by posterior humeral head subluxation and/ or varying degrees of posterior glenoid wear, as described with types B1, B2, and B3. Type B2 glenoid morphology refers to glenoid biconcavity (described further below), which has been shown to be associated with the highest rate of surgical complications [18]. Type C glenoids are congenital, characterized by dysplastic retroversion not caused by erosion [19]. Type D glenoids are characterized by glenoid anteversion and/or anterior humeral head subluxation.

Further additions to the Walch classification system have also been proposed, such as the type E glenoid morphologies of cuff tear arthropathy [15]. However, cuff tear arthropathy is a separate entity from glenohumeral osteoarthritis with intact rotator cuff. This discussion focuses on the latter, for which the modified Walch system of 2016 remains the primary classification scheme of interest. (Note that even in the absence of cuff tears, the status of the rotator cuff can impact glenoid morphology. For example, Donohue et al. [20] found that

Table 1 Modified Walch classification [17]. Quoted excerpts reprinted from *Journal of Shoulder and Elbow Surgery*, Vol. 25, Bercik MJ, Kruse K, Yalizis M, Gauci MO, Chaoui J, Walch G, "A modification to the Walch classification of the glenoid in primary glenohumeral osteoarthritis using three-dimensional imaging," pp. 1601–1606, Copyright 2016, with permission from Elsevier

Classification	Definition
A1	"Centered humeral head, minor erosion"
A2	"Centered humeral head, major central glenoid erosion"
B1	"Posterior subluxated head, no bony erosion"
B2	"Posterior subluxated head, posterior erosion with biconcavity of the glenoid"
B3	"Monoconcave and posteriorly worn, with at least 15° of retroversion or at least 70% posterior humeral head subluxation, or both"
C	"Dysplastic glenoid with at least 25° of retroversion not caused by erosion"
D	"Any level of glenoid anteversion or with [anterior] humeral head subluxation of less than 40%"

high-grade fatty muscle infiltration of the rotator cuff was associated with type B3 glenoid morphology.) The key bony changes of glenohumeral osteoarthritis with intact rotator cuff are reviewed next along with specific measures for quantifying these changes.

2D, corrected 2D and 3D measurement techniques

Measurement techniques may be classified as either 2D, corrected 2D (also sometimes referred to as "3D corrected"), or 3D techniques. 2D techniques refer to measurements taken in an ordinal imaging plane, not adjusted for the orientation of the scapula within the image. However, such measurements have been found to be subject to variation based on patient positioning within the scanner. This is addressed by re-orienting the imaging planes to the anatomic axes of the scapula using three reference points [21, 22]: the junction of the scapular spine and the medial scapular margin; the midpoint of the glenoid face; and the inferior-most tip of the scapula (Fig. 5). The corrected coronal plane passes through all three reference points. The corrected axial plane is perpendicular to the corrected coronal plane, and passes through the first two reference points. The corrected sagittal plane is perpendicular to both corrected coronal and corrected axial planes. By correcting the imaging planes in this way, measurements are made more anatomic with respect to the scapula, and dependence on patient positioning within the scanner is reduced. The use of corrected axial images has been shown to be more accurate than non-corrected images [23–26].

3D measurement techniques, on the other hand, rely on the manipulation of structures in three-dimensional space. Three specific 3D measures of the glenoid (i.e., the volumetric vault method for quantifying bone stock, the fitted-sphere method for measuring glenoid orientation, and surface area measures of biconcavity) have been developed, as described further below. Corrected 2D measurements generally remain the most practical metrics. Oblique multiplanar reconstruction tools are widely available on standard PACS and advanced visualization systems, and allow users to quickly re-orient images to the anatomic planes of the scapula.

Central bone loss

Bony wear at the central aspect of the glenoid leads to medialization of the joint line, and reduction of the bone stock available for support and fixation of a glenoid component. Such central loss may be mild (i.e., type A1, Fig. 4a) or more pronounced (i.e., type A2, Fig. 4b). In order to distinguish between A1 and A2 glenoids, a line joining the anterior and posterior margins of the glenoid is drawn. Type A2 glenoids are defined by the medial margin of the humeral head crossing this line.

The degree of central bone loss may be quantified using the depth of the glenoid vault. While the literature describes some variation in the methods of vault depth measurement (see for example [27–31]), a common strategy is to measure the depth from the center of the glenoid on a corrected axial image, along the Friedman line (a line joining the center of the glenoid with the medial margin of the scapula, as also described further below), to the far underlying endosteal margin (Fig. 6a).

Three-dimensional models of the glenoid vault have been proposed as a more comprehensive, volumetric method for quantifying glenoid bone loss. These methods involve the comparison of the affected glenoid with some premorbid estimate of the glenoid vault. That premorbid estimate may be derived from a normal contralateral glenoid in a specific patient [34] or from a statistical model based on many normal glenoids [35, 36]. However, such methods may require detailed manual delineation of vault margins and/or specialized software, and three-dimensional vault models have not yet entered widespread clinical use.

Posterior bone loss

Eccentric load bearing at the posterior aspect of the glenoid causes joint space narrowing and disproportionate bone thinning posteriorly (Fig. 4e). Posterior glenoid bone loss can lead to altered biomechanics with associated static posterior subluxation of the humeral head [37]. Preoperative posterior subluxation has been shown to produce inferior outcomes in total
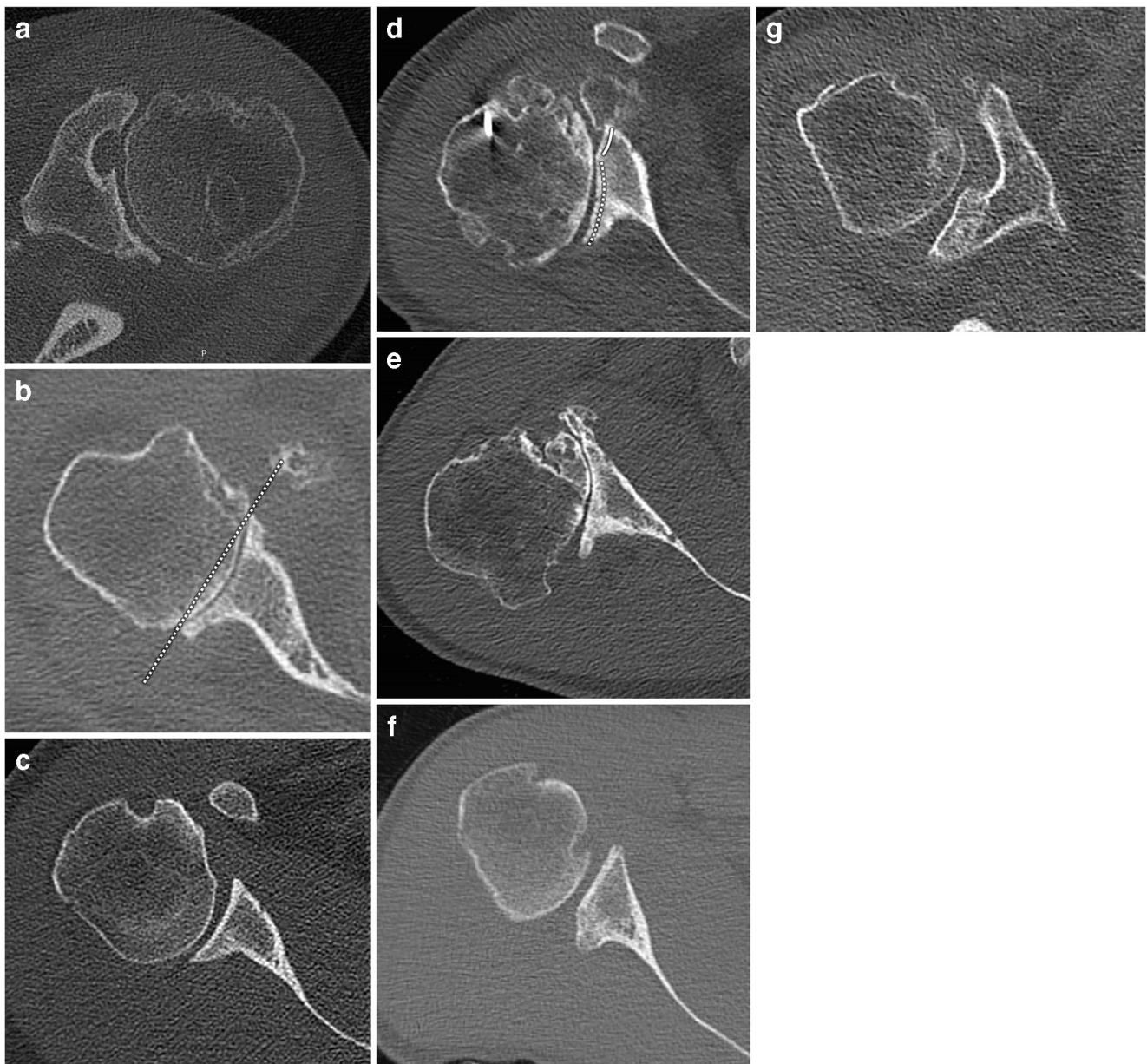
Fig. 4 Axial CT images from different patients illustrating the modified Walch glenoid classification system. **a** 67-year-old man with mild central glenoid erosion and a centered humeral head indicating an A1 glenoid. **b** 84-year-old man with prominent central glenoid erosion and a centered humeral head, consistent with A2 glenoid. Note that the articular surface of the humeral head crosses a line joining the anterior and posterior glenoid rim (dotted line), which distinguishes the A2 glenoid from A1. **c** 47-year-old man with posterior subluxation of the humeral head without bony erosion of the glenoid, consistent with B1 glenoid. **d** 68-year-old man with B2 glenoid exhibiting posterior subluxation of the humeral head with glenoid biconcavity. Disproportionate bony wearing at the posterior glenoid leads to the formation of a second articular facet (i.e., neoglenoid, dotted line), with a small residual facet of the native glenoid (i.e., paleoglenoid, solid line). **e** 78-year-old man with posterior bone loss leading to a monoconcave glenoid, and retroversion greater than 15 degrees, consistent with B3 glenoid. **f** 26-year-old man with congenitally dysplastic posterior glenoid with retroversion corresponding to type C glenoid. **g** 70-year-old man with anterior subluxation of the humeral head indicating type D glenoid

shoulder arthroplasty, though morphologic correction of the glenoid and soft tissue stabilization can lead to durable results [38]. Eccentric posterior bone loss may be quantified using linear measurements. Here, in contrast to the situation with central bone loss, the objective is to measure how much the posterior portion of the glenoid has been worn relative to the anterior glenoid [31, 39, 40]. A line is drawn through the anterior margin of the glenoid on a corrected axial image, perpendicular to the Friedman line. The greatest distance from this perpendicular line to the posterior glenoid represents a measure of posterior bone loss (Fig. 6b). Note also that
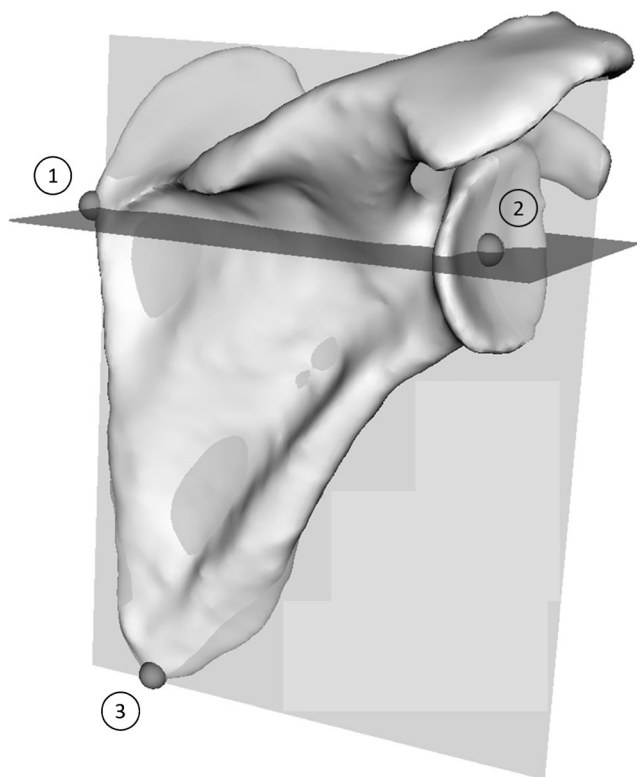
Fig. 5 Anatomic planes of the scapula. In order to correct for patient positioning during image acquisition, three reference points are used to define the anatomic planes of the scapula (gray spherical markers): (1) the junction of the scapular spine with the medial margin of the scapula, (2) the center of the glenoid, and (3) the inferior tip of the scapula. The corrected coronal plane passes through all three of these points (light gray plane). The corrected axial plane (dark gray plane) is perpendicular to the corrected coronal plane, and passes through points (1) and (2). The corrected sagittal plane (not shown) is perpendicular to both the corrected coronal and corrected axial planes. Standard oblique multiplanar reconstruction tools may be used to correct isotropic images to the anatomic planes of the scapula

posterior bone loss is closely associated with glenoid retroversion and biconcavity, discussed in detail below.

Related work has been done on quantifying bony deficiency in the setting of glenohumeral instability [41–44]. However, these measures are primarily designed to quantify bony defects, such as from traumatic injury, rather than the bony wearing of osteoarthritis. On the other hand, just as glenoid vault models have been used to measure central bone loss, the vault method may also be used to quantify eccentric posterior bone loss, although the same limitations apply as discussed above.

Retroversion

Disproportionate posterior glenoid bone loss often leads to alteration in glenoid version. The conventional measure of glenoid version is evaluated on an axial image through the mid glenoid [45]. Figure 6c shows version measurement on a corrected axial image. A line is drawn joining the midpoint

of the glenoid with the medial border of the scapula (i.e., the Friedman line). A perpendicular to this line represents neutral version. The angle of version is then defined as the angle between the line of neutral version and a line across the anterior and posterior margins of the glenoid (excluding osteophytes). Normal glenoid version measures approximately 0°, with the normal range varying between 2° of anteversion and 9° of retroversion in one study [46].

Inclination

Eccentric glenoid bone loss in the coronal plane is also an important factor. In anatomic TSA, glenoid component malpositioning in the coronal plane is associated with higher failure rate compared to malpositioning in the anteroposterior dimension [47]. In reverse TSA, superior bone loss can result in undesired superior angulation of the baseplate [33]. Glenoid bone loss in the coronal plane may be characterized using the glenoid inclination angle (Fig. 6d) [32, 33]. Using corrected coronal images as described above, the coronal image showing the glenoid in greatest profile is selected. On this image, a line along the floor of the supraspinatus fossa is drawn (i.e., the bottom of the trough-shaped fossa). The angle between this line, and a line joining the superior and inferior glenoid margins (excluding osteophytes), represents glenoid

Fig. 6 Preoperative measurements. **a** 42-year-old man. Corrected axial CT image (see text, and Fig. 5) illustrating glenoid vault depth (dotted arrow), which may be measured as the distance from the midpoint of the glenoid, along the Friedman line (see text and Fig. 6(c)) to the far underlying endosteal surface. **b** 70-year-old man with corrected axial CT image demonstrating bony thinning at the posterior glenoid. Starting with the Friedman line (dashed), a perpendicular line (solid) is drawn through the anterior margin of the glenoid, excluding osteophytes. Posterior bone loss may then be measured as the greatest distance from that perpendicular to the glenoid (dotted arrow). **c** 45-year-old man with glenoid retroversion measuring 12 degrees on corrected axial CT. A line is drawn between the midpoint of the glenoid and the medial margin of the scapula (i.e., the Friedman line; dashed line with circular white endpoints). The perpendicular to this axis represents neutral version (solid). Glenoid version is then defined as the angle (α) between the line of neutral version, and a line across the anterior and posterior glenoid margins, excluding osteophytes (dotted). **d** 67-year-old man with normal glenoid inclination measuring 75 degrees on corrected coronal CT. A line is drawn across the glenoid fossa (solid line). A second line is drawn along the floor (inferior cortical margin) of the supraspinatus fossa. The angle between these lines (β) is the glenoid inclination [32]. Note, however, that other authors report glenoid inclination as 90 degrees minus β [33]. **e** 28-year-old man with a centered humeral head on corrected axial CT. The glenohumeral index measures humeral head subluxation, and reflects the proportion of the humeral head posterior to a line bisecting the glenoid. A line is drawn joining the anterior and posterior glenoid margins, excluding osteophytes (solid). A perpendicular line is then drawn which divides the glenoid in half (dashed). A diameter across the medial third of the humeral head is then divided into two portions (dotted arrows), an anterior portion x_{ant} and a posterior portion x_{post}. The glenohumeral index is defined as $x_{post}/(x_{ant} + x_{post})$
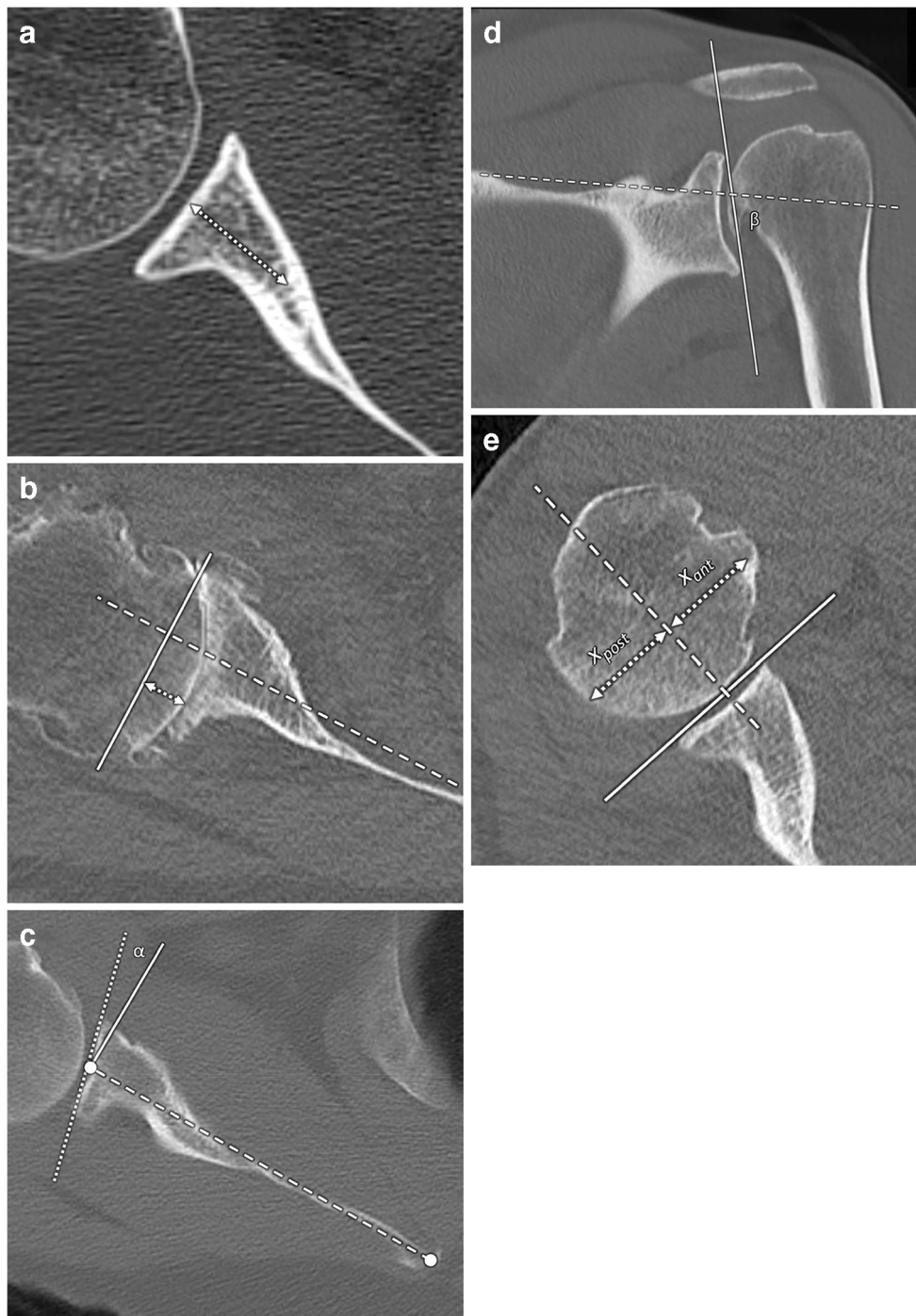
inclination. (Note that some authors report glenoid inclination as 90 degrees minus this angle [33].) When coronal plane glenoid bone loss occurs in the setting of cuff tear arthropathy, we refer the reader elsewhere with regard to type E glenoid morphologies [15].

With regard to both glenoid version and glenoid inclination, three-dimensional techniques have been developed for quantifying these measures [22, 48–50]. These methods use a spherical surface fitted to the glenoid face. The radial ray from the center of the fitted sphere, to the center of the glenoid, serves as an overall indicator of the orientation of the glenoid face in three dimensions. Version (i.e., the orientation in the corrected axial plane) and inclination (i.e., the orientation in the corrected coronal plane) may then be derived from this radial ray by projection into the corrected axial and coronal planes, respectively. As with the glenoid vault method for volumetric bone stock analysis, however, these fitted-sphere methods currently rely on proprietary or research implementations not widely available.

Biconcavity

Posterior load bearing and bone loss may lead to the formation of a second concave surface at the glenoid that entrenches the posteriorly subluxed humeral head, corresponding to type B2 glenoid morphology (Fig. 4d). The new posterior concavity is called the neoglenoid while the native anterior articular surface remnant is the paleoglenoid. Such biconcavity alters glenohumeral biomechanics, further exacerbating posterior load bearing. The size of the neoglenoid is important in preoperative planning in choosing between eccentric reaming with a standard glenoid component for milder deformity, or for more severe deformity, either bone grafting with a standard component, or an augmented component (see below) [51]. The degree of posterior humeral head subluxation also affects the choice of implant type, including selection of reverse versus anatomic arthroplasty. Humeral head positioning with respect to the glenoid can be measured with the glenohumeral index, which reflects the proportion of the humeral head posterior to a line bisecting the glenoid (Fig. 6e). The glenohumeral index is 45–55% for a centered humeral head, more than 55% for posterior subluxation, and less than 45% for anterior subluxation [16, 52]. Biconcavity may also be assessed by evaluating the surface areas of the neoglenoid and paleoglenoid [53], and humerus-subtracted volume rendering [54] may be used for visual estimation of the relative surface areas (Fig. 7). In addition, the version of the
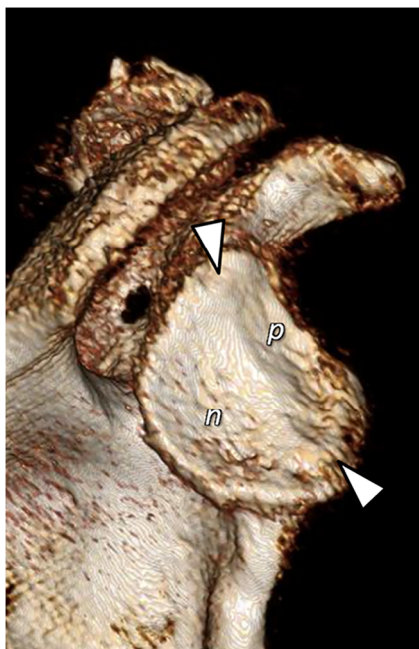

Fig. 7 62-year-old man with glenoid biconcavity consistent with Walch B2 morphology. Humerus-subtracted volume rendering of the glenoid shows the paleoglenoid (*p*) and the neoglenoid (*n*), which meet along a ridge (endpoints marked with arrowheads). Relative surface area can be estimated by visual inspection, with the area of the paleoglenoid representing approximately 40% and the neoglenoid approximately 60% of the overall glenoid surface area

neoglenoid has also been described as another method for characterizing B2 glenoids [39].

Osteophytes

Preoperative imaging demonstrates the location and size of glenohumeral osteophytes, which are important for several reasons. Glenoid osteophytes may obscure the true margins of the glenoid and may bias version measurement, and osteophytes are typically excluded from the glenoid margin in orientation measurements [45, 50]. Posterior glenoid osteophytes (and posterior humeral neck osteophytes) can tension the posterior joint capsule, interfering with intraoperative glenoid exposure by making it more difficult to subluxate the humerus posteriorly. Large inferior glenoid osteophytes can limit retraction of the humerus inferiorly [55]. Anterior glenoid osteophytes can impede accurate placement of the central guide pin and cause the pin to be inserted in too much retroversion [51]. Overall, characterization of the size and location of glenoid osteophytes informs the surgical approach, operative exposure, and component placement.

Subchondral bone quality

Shear and compressive forces at the glenohumeral joint are better resisted by dense cortical bone than trabeculated cancellous bone. Preservation of dense subchondral bone at the glenoid is recognized as an important factor in glenoid component durability [56, 57]. Excessive removal of subchondral bone has been shown to lead to higher rates of aseptic loosening [58]. Particularly for the aTSA, it is critical to preserve as much of the subchondral bone to decrease micromotion at the bone-implant interface [59]. The thickness of the subchondral cortical bone has been measured as one relevant indicator [57]. As a related issue, the presence of subchondral cysts (i.e., geodes) may also influence surgical planning, by requiring further surface preparation or repair [60].

Bone density

Regarding bone density, extensive work has been done in the area of quantitative CT, which involves the conversion of x-ray attenuation information into bone mineral density (BMD) data. These techniques may utilize phantom-based calibration, tissue-based calibration, or dual-energy methods [61–64]. While much of this work has focused on the spine and hip, BMD at the glenoid has been studied as a factor in glenoid component durability. A cadaveric study found that lower BMD as measured with quantitative CT was associated with greater mechanical displacement of a glenoid prosthesis [65]. In another cadaveric study, glenoid BMD and other measures of trabecular architecture were assessed using quantitative CT techniques [66]. However, in the absence of formal

quantitative CT for BMD assessment, the use of Hounsfield units from clinical CT imaging has been advocated as a readily available estimate of bone density [67–70].

Surgical techniques at the glenoid

Several surgical techniques are available to the surgeon in order to optimize glenoid component implantation and to maximize the long-term success of the total shoulder arthroplasty. With each of these techniques, a fundamental objective is to achieve accurate placement and optimal seating of the glenoid component, while restoring glenoid version and preserving as much of the glenoid bone stock as possible for structural support. The selection of specific techniques depends on morphological characterization of the glenoid at pre-operative imaging.

Eccentric reaming

Glenoid reaming is a common technique used to correct retroversion in asymmetric posterior glenoid bone loss and to prepare the glenoid surface for placement of the glenoid component. The goal is to minimize edge loading which causes component loosening at the glenoid in anatomic TSA, particularly in those with B2 glenoids. After exposure of the glenoid surface and placement of a central guide pin, a glenoid resurfacing reamer (a rotational burring device) is slid over the guide pin. The anterior high side of the glenoid is then reamed toward the level of the posterior glenoid surface, thus correcting the glenoid version (Fig. 8).

In exchange for corrected version, eccentric reaming sacrifices dense cortical bone anteriorly and causes medialization of the joint line, altering biomechanics by shifting the center of rotation. Minor retroversion can be corrected with eccentric reaming to restore normal glenoid version. In retroversion greater than 15°, use of reaming to achieve satisfactory glenoid component positioning is difficult without excessive bone removal, and also presents a high risk of peg penetration of the glenoid vault leading to fixation failure [71, 72]. When penetration occurs, extruded cement can cause injury or compression of the suprascular nerve as it courses through the spinoglenoid notch [3, 73]. For these patients, bone grafting with a standard component or use of an augmented component may be appropriate (see below). In retroversion greater than 20°, reverse TSA may be a last resort, due to high rates of anatomic TSA failure. When compared to anatomic TSA, reverse TSA in these patients has been shown to demonstrate decreased glenoid component loosening and improved functional outcomes in the early stages [54, 74, 75].
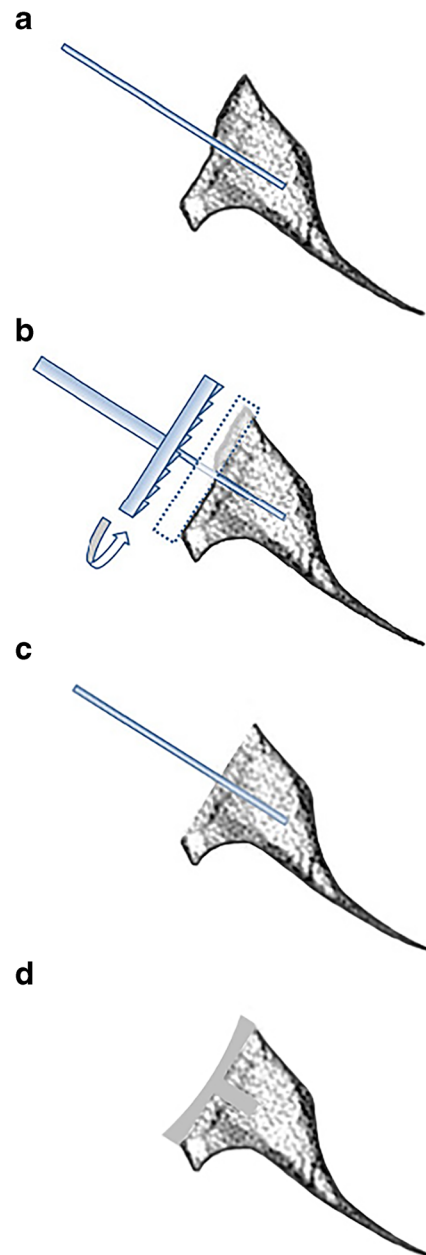

Fig. 8 Eccentric reaming of a B2 glenoid to correct biconcavity and retroversion. **a** First, a central pin is placed which serves as a guide for tool placement. **b** The reamer, which is a rotational burring device, is placed over this pin and advanced to remove the raised portion of the anterior glenoid (dotted box). **c**, **d** This leaves a planarized glenoid margin, with correction of the native biconcavity and retroversion, for subsequent glenoid component placement. However, reaming removes bone, especially dense cortical bone, when bone stock is already limited. Reaming also medializes the margin of the glenoid, which alters biomechanics

Bone grafting

Alternatively, restoring glenoid version may be achieved by augmenting the native glenoid bone with autograft or allograft material (Fig. 9). This approach allows for glenoid version correction without eccentric reaming, thus preserving the
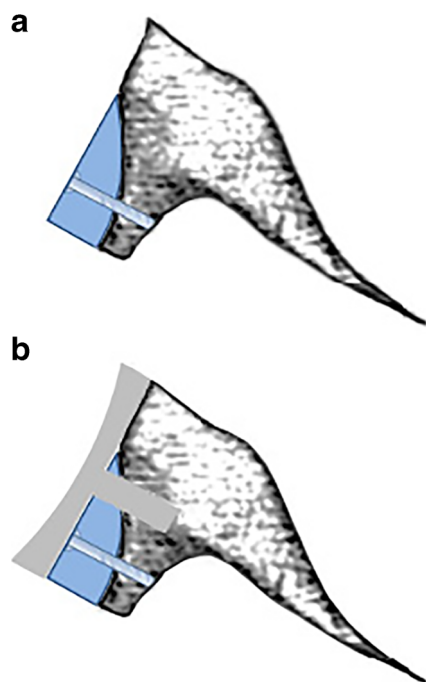
Fig. 9 Bone grafting in a B2 glenoid with more severe posterior bone loss. Bone grafting is an alternate approach to correcting posterior bone loss and retroversion. Instead of anterior bone removal as with eccentric reaming, here bone material is added posteriorly to correct biconcavity and retroversion. a Bone graft material is placed at the posterior glenoid and fixed to the native bone with screws. b Glenoid component placement may then be performed. While bone grafting augments bone stock rather than subtracting from it, the use of bone grafting presents its own challenges. This sometimes requires two surgeries (one for bone graft placement, and a second for component placement after graft healing has occurred). The degree of graft healing may also be incomplete.

anterior glenoid bone stock and avoiding medialization of the glenoid vault [76]. However, bone grafting is technically difficult and is associated with graft-related complications such as graft dissolution, nonunion, and fixation failure [2]. Total shoulder arthroplasties with bone grafting can be single stage procedures, or sometimes require two surgeries (one to place the bone graft and a second to perform the arthroplasty after graft healing has occurred). Autograft is typically harvested from the humeral head at initial arthroplasty, or from the iliac crest at revision arthroplasty. The graft is then contoured to fill the posterior glenoid defect. In general, no more than 40–50% of the glenoid component should be supported by bone graft. Bone grafting for anatomic TSA has achieved varying rates of success [18] and is now uncommonly performed. On the other hand, bone grafting for reverse TSA is frequently used and has been reported to provide better functional outcomes [77, 78].

Eccentric reaming with bone graft

Bone grafting can also be performed in conjunction with partial reaming to correct glenoid retroversion (Fig. 10). Similar to bone grafting alone, this combination of techniques is more
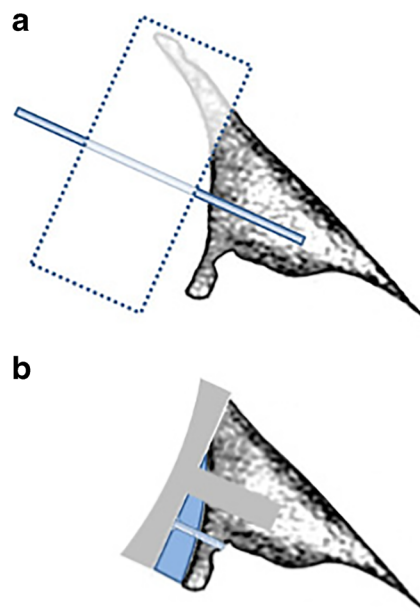

Fig. 10 Eccentric reaming and bone grafting to correct a B3 monoconcave glenoid. In cases of severe posterior bone loss, eccentric reaming and bone grafting may be applied in combination. a Partial eccentric reaming, with removal of a portion of the anterior glenoid (dotted box), serves to partially correct glenoid version. b This leaves an area of residual posterior bony deficiency, which can be corrected with a bone graft, enabling subsequent glenoid component placement

commonly performed for reverse than anatomic arthroplasties. The central guide pin is first placed along the glenoid axis, allowing for limited reaming of the anterior high side. The residual posterior defect is then prepared to receive the bone graft using an angled reamer. This approach avoids excessive reaming, conserves glenoid bone stock, and limits medialization of the joint line.

Augmented glenoid components

As a relatively new prosthetic solution to correcting glenoid version in posterior glenoid bone loss, augmented glenoid components for anatomic TSA provide an alternative to eccentric reaming and bone grafting. Here, the glenoid component itself is augmented posteriorly, to compensate for disproportionate posterior bone deficiency. Aside from minimizing bone loss from excessive reaming, this technique also avoids the complications related to bone grafting. The augmented portion of the glenoid component may be step-cut, half-wedged, or full-wedged in shape (Fig. 11). Prior to component placement, the glenoid is typically prepared with reaming to achieve optimal seating [79–81]. In addressing B2 glenoids, half-wedged augments require the least amount of bone removal to correct glenoid version and inclination, thus preserving the dense anterior cortical bone for implant stability [51, 82]. In contrast, a full-wedged augment may be more suitable for a B3 glenoid to help account for the medialization associated with this morphology. Although mid- and long-term

survivorship data is not yet available, current literature shows promising short-term results for the management of B2 and B3 glenoids with augmented glenoid components [83, 84].
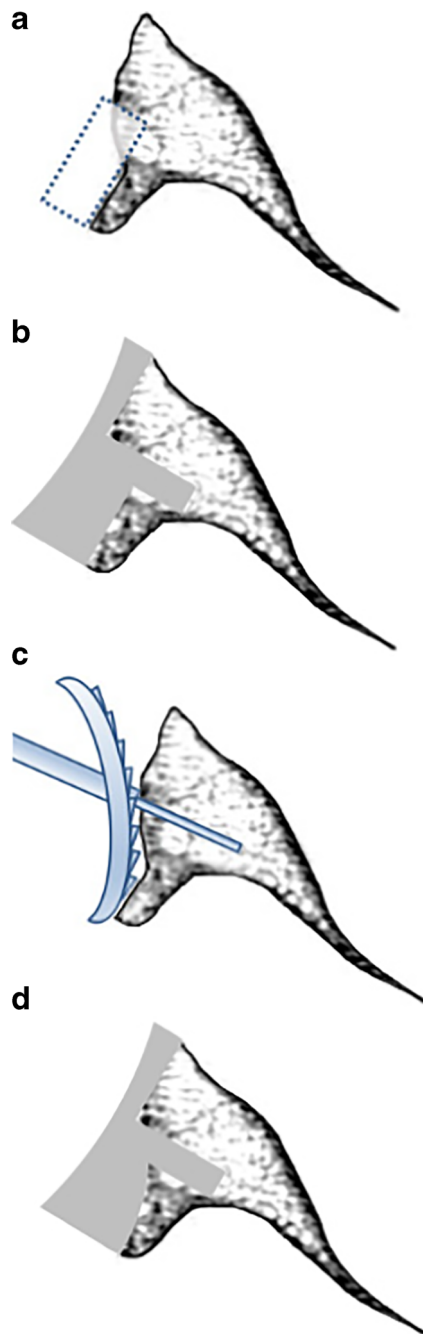

Fig. 11 Augmented glenoid components. More recently, augmentation of the glenoid component has been introduced as another means by which to compensate for posterior glenoid bone loss. **a, b** In the case of step-shaped augmentation, a block-shaped corner is cut from the posterior glenoid, corresponding to the stepped contour of the device. **c, d** Alternatively, for devices with wedge-shaped augmentation, the posterior facet of a biconcave glenoid is prepared with angled reaming, conforming to the angled surface of the glenoid component

Reverse instead of anatomic TSA

The reverse TSA (Fig. 12a) was initially designed to address CTA with an irreparable rotator cuff. As the indications for reverse TSA have expanded, reverse TSA has become a treatment option for osteoarthritis in select patients with significant posterior glenoid bone loss, typically with a surgeon-dependent lower limit on patient age. Particularly for B2 glenoids, anatomic TSA may be difficult in cases presenting with excessive glenoid retroversion and posterior humeral head subluxation, even with techniques such as eccentric reaming, bone grafting, or augmented glenoid components. Several studies have supported the use of reverse TSA in glenohumeral osteoarthritis despite an intact rotator cuff, especially given the relatively high rate of early glenoid component loosening in anatomic TSA for severe retroversion [74, 75, 85–86].

When needed, the reverse TSA baseplate may be lateralized using a bony or metal augment (Fig. 12b). This
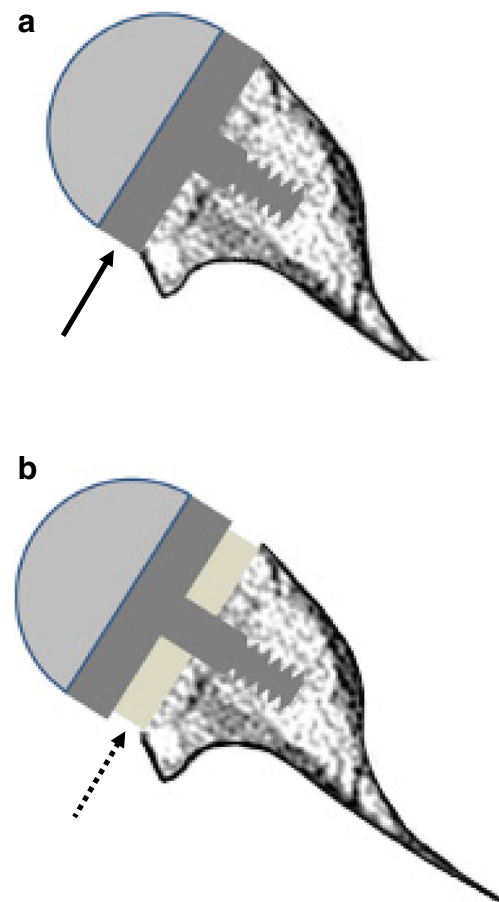

Fig. 12 Glenoid component of reverse total shoulder arthroplasty. **a** The glenoid component of reverse TSA consists of a baseplate (metaglene, solid arrow) fixed to the glenoid, and a convex articulating component (glenosphere, light gray) attached to the baseplate. **b** If the glenoid has been excessively medialized, augmentation (dotted arrow) beneath the metaglene may be used

may correct for deficiency of the native bone, or surgical bone removal, and limits complications such as scapular notching [15, 87, 88]. Although more evidence is needed to demonstrate the long-term efficacy of reverse TSA for indications other than CTA with an irreparable rotator cuff, reverse TSA has gained increasing popularity for restoring function and alleviating pain in older patients with severe retroversion. Reverse TSA has also been shown to lead to short-term functional improvements in younger patients (i.e., less than or equal to 65 years of age) [89–91]. However, many surgeons are reluctant to perform reverse TSA on younger patients when much of the data has yet to be collected for long-term implant survivability.

Conclusion

The glenoid side of the shoulder joint is widely recognized as a primary limitation in the long-term durability of shoulder arthroplasty. A variety of surgical techniques may be used to manage the glenoid at shoulder arthroplasty. Understanding the nature and severity of glenoid deformity is essential for surgical planning. The modified Walch classification system is a key part of describing glenoid morphologies including central bone loss, posterior bone loss, retroversion, and biconcavity. Other important morphologic factors include glenoid inclination, glenohumeral osteophytes, subchondral bone quality, and bone density. Re-orienting isotropic CT images to the anatomic planes of the scapula serves to correct for patient positioning and allows for more accurate morphologic measurements. Humerus-subtracted volume rendering is also a useful visualization technique. Ultimately, a primary surgical objective is to correct glenoid deformity while preserving bone stock. Selection of surgical techniques for a given patient depends critically on the characterization of glenoid morphology at pre-operative imaging.

Compliance with ethical standards

Conflict of interest Dr Lo has nothing to disclose. Dr. Leong has nothing to disclose. Dr. Shiu reports personal fees from Zimmer/Biomet during the conduct of the study. Dr. Gilotra reports speaking fees from Arthrex outside the submitted work. Dr. Wang reports other relationships with DexNote LLC, and University of California San Francisco, outside the submitted work. In addition, Drs. Gilotra, Hasan, Koenig and Wang have a patent pending regarding shoulder ultrasound.

References

1. Palsis JA, Simpson KN, Matthews JH, Traven S, Eichinger JK, Friedman RJ. Current trends in the use of shoulder arthroplasty in the United States. Orthopedics. 2018;41(3):416–23.

2. Sears BW, Johnston PS, Ramsey ML, Williams GR. Glenoid bone loss in primary total shoulder arthroplasty: evaluation and management. J Am Acad Orthop Surg. 2012;20(9):604–13.

3. Pinkas D, Wiater B, Wiater JM. The glenoid component in anatomic shoulder arthroplasty. J Am Acad Orthop Surg. 2015;23(5):317–26.

4. Boileau P. Complications and revision of reverse total shoulder arthroplasty. Orthop Traumatol Surg Res. 2016;102(1):S33–43.

5. Rojas J, Choi K, Joseph J, Srikumaran U, McFarland EG. Aseptic glenoid baseplate loosening after reverse total shoulder arthroplasty: a systematic review and meta-analysis. JBJS Rev. 2019;7(5):1–7.

6. Bohsali KI, Bois AJ, Wirth MA. Complications of shoulder arthroplasty. J Bone Joint Surg Am. 2017;99(3):256–69.

7. McLendon PB, Schoch BS, Sperling JW, Sánchez-Sotelo J, Schleck CD, Cofield RH. Survival of the pegged glenoid component in shoulder arthroplasty: part II. J Shoulder Elb Surg. 2017;26(8):1469–76.

8. Papadonikolakis A, Matsen FA. Metal-backed glenoid components have a higher rate of failure and fail by different modes in comparison with all-polyethylene components: a systematic review. J Bone Joint Surg Am. 2014;96(12):1041–7.

9. Lo IK, Litchfield RB, Griffin S, Faber K, Patterson SD, Kirkley A. Quality-of-life outcome following hemiarthroplasty or total shoulder arthroplasty in patients with osteoarthritis. J Bone Joint Surg Am. 2005;87(10):2178–85.

10. Gartsman GM, Roddey TS, Hammerman SM. Shoulder arthroplasty with or without resurfacing of the glenoid in patients who have osteoarthritis. J Bone Joint Surg Am. 2000;82(1):26–34.

11. Lazarus MD, Jensen KL, Southworth C, Matsen FA. The radiographic evaluation of keeled and pegged glenoid component insertion. J Bone Joint Surg Am. 2002;84(7):1174–82.

12. Collin P, Tay AK, Melis B, Boileau P, Walch G. A ten-year radiologic comparison of two-all polyethylene glenoid component designs: a prospective trial. J Shoulder Elb Surg. 2011;20(8):1217–23.

13. Melis B, DeFranco M, Lädermann A, et al. An evaluation of the radiological changes around the Grammont reverse geometry shoulder arthroplasty after eight to 12 years. J Bone Joint Surg (Br). 2011;93(9):1240–6.

14. Lädermann A, Schwitzguebel AJ, Edwards TB, et al. Glenoid loosening and migration in reverse shoulder arthroplasty. Bone Joint J. 2019;101(4):461–9.

15. Sirveaux F, Favard L, Oudet D, Huquet D, Walch G, Mole D. Grammont inverted total shoulder arthroplasty in the treatment of glenohumeral osteoarthritis with massive rupture of the cuff: results of a multicentre study of 80 shoulders. J Bone Joint Surg (Br). 2004;86(3):388–95.

16. Walch G, Badet R, Boulahia A, Khoury A. Morphologic study of the glenoid in primary glenohumeral osteoarthritis. J Arthroplast. 1999;14(6):756–60.

17. Bercik MJ, Kruse K, Yalizis M, Gauci MO, Chaoui J, Walch G. A modification to the Walch classification of the glenoid in primary glenohumeral osteoarthritis using three-dimensional imaging. J Shoulder Elb Surg. 2016;25(10):1601–6.

18. Gates S, Cutler H, Khazzam M. Outcomes of posterior glenoid bone-grafting in anatomical total shoulder arthroplasty: a systematic review. JBJS Rev. 2019;7(9):e6.

19. Harper KW, Helms CA, Haystead CM, Higgins LD. Glenoid dysplasia: incidence and association with posterior labral tears as evaluated on MRI. AJR Am J Roentgenol. 2005;184(3):984–8.

20. Donohue KW, Ricchetti ET, Ho JC, Iannotti JP. The association between rotator cuff muscle fatty infiltration and glenoid morphology in glenohumeral osteoarthritis. J Bone Joint Surg Am. 2018;100(5):381–7.

21. Kwon YW, Powell KA, Yum JK, Brems JJ, Iannotti JP. Use of three-dimensional computed tomography for the analysis of the glenoid anatomy. J Shoulder Elb Surg. 2005;14(1):85–90.

22. Lewis GS, Armstrong AD. Glenoid spherical orientation and version. J Shoulder Elb Surg. 2011;20(1):3–11.

23. Bokor DJ, O'Sullivan MD, Hazan GJ. Variability of measurement of glenoid version on computed tomography scan. J Shoulder Elb Surg. 1999;8(6):595–8.

24. Budge MD, Lewis GS, Schaefer E, Coquia S, Flemming DJ, Armstrong AD. Comparison of standard two-dimensional and three-dimensional corrected glenoid version measurements. J Shoulder Elb Surg. 2011;20(4):577–83.

25. Petscavage JM, Ha AS, Chew FS. Current concepts of shoulder arthroplasty for radiologists: part 1–epidemiology, history, preoperative imaging, and hemiarthroplasty. AJR Am J Roentgenol. 2012;199(4):757–67.

26. Chalmers PN, Salazar D, Chamberlain A, Keener JD. Radiographic characterization of the B2 glenoid: the effect of computed tomographic axis orientation. J Shoulder Elb Surg. 2017;26(2):258–64.

27. Roberts CC, Ekelund AL, Renfree KJ, Liu PT, Chew FS. Radiologic assessment of reverse shoulder arthroplasty. Radiographics. 2007;27(1):223–35.

28. Codsi MJ, Bennetts C, Gordiev K, et al. Normal glenoid vault anatomy and validation of a novel glenoid implant shape. J Shoulder Elb Surg. 2008;17(3):471–8.

29. Poon PC, Ting FS. A 2-dimensional glenoid vault method for measuring glenoid version on computed tomography. J Shoulder Elb Surg. 2012;21(3):329–35.

30. Damas CN, Silva J, Sá MC, Torres J. Computed tomography morphological analysis of the scapula and its implications in shoulder arthroplasty. Eur J Orthop Surg Traumatol. 2016;26(2):127–32.

31. Siebert MJ, Chalian M, Sharifi A, Pezeshk P, Xi Y, Lawson P, et al. Qualitative and quantitative analysis of glenoid bone stock and glenoid version: inter-reader analysis and correlation with rotator cuff tendinopathy and atrophy in patients with shoulder osteoarthritis. Skelet Radiol. 2020;49(6):985–93.

32. Maurer A, Fucentese SF, Pfirrmann CW, et al. Assessment of glenoid inclination on routine clinical radiographs and computed tomography examinations of the shoulder. J Shoulder Elb Surg. 2012;21(8):1096–103.

33. Favard L, Berhouet J, Walch G, Chaoui J, Lévigne C. Superior glenoid inclination and glenoid bone loss: Definition, assessment, biomechanical consequences, and surgical options. Orthopade. 2017;46(12):1015–21.

34. Scalise JJ, Bryan J, Polster J, Brems JJ, Iannotti JP. Quantitative analysis of glenoid bone loss in osteoarthritis using three-dimensional computed tomography scans. J Shoulder Elb Surg. 2008;17(2):328–35.

35. Abler D, Berger S, Terrier A, Becce F, Farron A, Büchler P. A statistical shape model to predict the premorbid glenoid cavity. J Shoulder Elb Surg. 2018;27(1):1800–8.

36. Plessers K, Verhaegen F, Van Dijck C, et al. Automated quantification of glenoid bone defects using 3-dimensional measurements. J Shoulder Elb Surg. 2020;29(5):1050–8.

37. Hsu JE, Ricchetti ET, Huffman GR, Iannotti JP, Glaser DL. Addressing glenoid bone deficiency and asymmetric posterior erosion in shoulder arthroplasty. J Shoulder Elb Surg. 2013;22(9):1298–308.

38. Gerber C, Costouros JG, Sukthankar A, Fucentese SF. Static posterior humeral head subluxation and total shoulder arthroplasty. J Shoulder Elb Surg. 2009;18(4):505–10.

39. Churchill RS, Spencer EE, Fehringer EV. Quantification of B2 glenoid morphology in total shoulder arthroplasty. J Shoulder Elb Surg. 2015;24(8):1212–7.

40. Lanzetti RM, Spoliti M. A new geometric model to quantify the area of glenoid bone defect and medialisation of the native joint line in glenohumeral arthritis. Eur J Orthop Surg Traumatol. 2019;29(6):1211–6.

41. Chuang TY, Adams CR, Burkhart SS. Use of preoperative three-dimensional computed tomography to quantify glenoid bone loss in shoulder instability. Arthroscopy. 2008;24(4):376–82.

42. Gyftopoulos S, Hasan S, Bencardino J, Mayo J, Nayyar S, Babb J, et al. Diagnostic accuracy of MRI in the measurement of glenoid bone loss. AJR Am J Roentgenol. 2012;199(4):873–8.

43. Altan E, Ozbaydar MU, Tonbul M, Yalcin L. Comparison of two different measurement methods to determine glenoid bone defects: area or width? J Shoulder Elb Surg. 2014;23(8):1215–22.

44. Beaulieu-Jones BR, Peebles LA, Golijanin P, et al. Characterization of posterior glenoid bone loss morphology in patients with posterior shoulder instability. Arthroscopy. 2019;35(10):2777–84.

45. Friedman RJ, Hawthorne KB, Genez BM. The use of computerized tomography in the measurement of glenoid version. J Bone Joint Surg Am. 1992;74(7):1032–7.

46. Strauss EJ, Roche C, Flurin PH, Wright T, Zuckerman JD. The glenoid in shoulder arthroplasty. J Shoulder Elb Surg. 2009;18(5):819–33.

47. Hopkins AR, Hansen UN, Amis AA, Emery R. The effects of glenoid component alignment variations on cement mantle stresses in total shoulder arthroplasty. J Shoulder Elb Surg. 2004;13(6):668–75.

48. Ghafurian S, Galdi B, Bastian S, Tan V, Li K. Computerized 3D morphological analysis of glenoid orientation. J Orthop Res. 2016;34(4):692–8.

49. Chan K, Knowles NK, Chaoui J, et al. Characterization of the Walch B3 glenoid in primary osteoarthritis. J Shoulder Elb Surg. 2017;26(5):909–14.

50. Boileau P, Cheval D, Gauci M-O, Holzer N, Chaoui J, Walch G. Automated three-dimensional measurement of glenoid version and inclination in arthritic shoulders. J Bone Joint Surg Am. 2018;100(1):57–65.

51. Donohue KW, Ricchetti ET, Iannotti JP. Surgical management of the biconcave (B2) glenoid. Curr Rev Musculoskelet Med. 2016;9(1):30–9.

52. Domos P, Checchia CS, Walch G. Walch B0 glenoid: pre-osteoarthritic posterior subluxation of the humeral head. J Shoulder Elb Surg. 2018;27(1):181–8.

53. Knowles NK, Keener JD, Ferreira LM, Athwal GS. Quantification of the position, orientation, and surface area of bone loss in type B2 glenoids. J Shoulder Elb Surg. 2015;24(4):503–10.

54. Wang KC, Jones A, Kambhampati S, et al. CT-based 3D printing of the glenoid prior to shoulder arthroplasty: bony morphology and model evaluation. J Digit Imaging. 2019;32(5):816–26.

55. Laver L, Garrigues GE. Avoiding superior tilt in reverse shoulder arthroplasty: a review of the literature and technical recommendations. J Shoulder Elb Surg. 2014;23(10):1582–90.

56. Knowles NK, Athwal GS, Keener JD, Ferreira LM. Regional bone density variations in osteoarthritic glenoids: a comparison of symmetric to asymmetric (type B2) erosion patterns. J Shoulder Elb Surg. 2015;24(3):425–32.

57. Simon P, Gupta A, Pappou I, et al. Glenoid subchondral bone density distribution in male total shoulder arthroplasty subjects with eccentric and concentric wear. J Shoulder Elb Surg. 2015;24(3):416–24.

58. Walch G, Young AA, Melis B, Gazielly D, Loew M, Boileau P. Results of a convex-back cemented keeled glenoid component in primary osteoarthritis: multicenter study with a follow-up greater than 5 years. J Shoulder Elb Surg. 2011;20(3):385–94.

59. Sowa B, Bochenek M, Braun S, et al. The subchondral bone layer and glenoid implant design are relevant for primary stability in glenoid arthroplasty. Arch Orthop Trauma Surg. 2018;138(11):1487–94.

60. Cofield RH, Sperling JW. Total shoulder replacement: managing bone deficiencies. In: Craig EV, editor. The shoulder. 3rd ed. Philadelphia: Lippincott Williams and Wilkins; 2013. p. 573–9.

61. Bauer JS, Henning TD, Müeller D, Lu Y, Majumdar S, Link TM. Volumetric quantitative CT of the spine and hip derived from contrast-enhanced MDCT: conversion factors. AJR Am J Roentgenol. 2007;188(5):1294–301.

62. Wichmann JL, Booz C, Wesarg S, et al. Dual-energy CT–based phantomless in vivo three-dimensional bone mineral density assessment of the lumbar spine. Radiology. 2014;271(3):778–84.

63. Brett AD, Brown JK. Quantitative computed tomography and opportunistic bone density screening by dual use of computed tomography scans. J Orthop Transl. 2015;3(4):178–84.

64. Knowles NK, Reeves JM, Ferreira LM. Quantitative computed tomography (QCT) derived bone mineral density (BMD) in finite element studies: a review of the literature. J Exp Orthop. 2016;3(1):36.

65. Chamseddine M, Breden S, Pietschmann MF, Müller PE, Chevalier Y. Periprosthetic bone quality affects the fixation of anatomic glenoids in total shoulder arthroplasty: in vitro study. J Shoulder Elb Surg. 2019;28(1):e18–28.

66. Jun BJ, Vasanji A, Ricchetti ET, et al. Quantification of regional variations in glenoid trabecular bone architecture and mineralization using clinical computed tomography images. J Orthop Res. 2018;36(1):85–96.

67. Schreiber JJ, Anderson PA, Rosas HG, Buchholz AL, Au AG. Hounsfield units for assessing bone mineral density and strength: a tool for osteoporosis management. J Bone Joint Surg Am. 2011;93(1):1057–63.

68. Cody EA, Lachman JR, Gausden EB, Nunley JA. Lower bone density on preoperative computed tomography predicts periprosthetic fracture risk in total ankle arthroplasty. Foot Ankle Int. 2019;40(1):1–8.

69. Pickhardt PJ, Graffy PM, Zea R, et al. Automated abdominal CT imaging biomarkers for opportunistic prediction of future major osteoporotic fractures in asymptomatic adults. Radiology. 2020;297(1):64–72.

70. Boutin RD, Lenchik L. Value-added opportunistic CT: insights into osteoporosis and sarcopenia. AJR Am J Roentgenol. 2020;215(3):582–94.

71. Gillespie R, Lyons R, Lazarus M. Eccentric reaming in total shoulder arthroplasty: a cadaveric study. Orthopedics. 2009;32(1):21.

72. Iannotti JP, Greeson C, Downing D, Sabesan V, Bryan JA. Effect of glenoid deformity on glenoid component placement in primary shoulder arthroplasty. J Shoulder Elb Surg. 2012;21(1):48–55.

73. Nové-Josserand L, Clavert P. Glenoid exposure in total shoulder arthroplasty. Orthop Traumatol Surg Res. 2018;104(1S):129–35.

74. Mizuno N, Denard PJ, Raiss P, Walch G. Reverse total shoulder arthroplasty for primary glenohumeral osteoarthritis in patients with a biconcave glenoid. J Bone Joint Surg Am. 2013;95(14):1297–304.

75. McFarland EG, Huri G, Hyun YS, Petersen SA, Srikumaran U. Reverse total shoulder arthroplasty without bone-grafting for severe glenoid bone loss in patients with osteoarthritis and intact rotator cuff. J Bone Joint Surg. 2016;98(21):1801–7.

76. Mehta SK, Aleem AW. Management of the B2 glenoid in glenohumeral osteoarthritis. Orthop Clin North Am. 2019;50(4):509–20.

77. Ernstbrunner L, Werthel JD, Wagner E, Hatta T, Sperling JW, Cofield RH. Glenoid bone grafting in primary reverse total shoulder arthroplasty. J Shoulder Elb Surg. 2017;26(8):1441–7.

78. Tashjian RZ, Broschinsky K, Stertz I, Chalmers PN. Structural glenoid allograft reconstruction during reverse total shoulder arthroplasty. J Shoulder Elb Surg. 2020;29(3):534–40.

79. Rice RS, Sperling JW, Miletti J, Schleck C, Cofield RH. Augmented glenoid component for bone deficiency in shoulder arthroplasty. Clin Orthop. 2008;466(3):579–83.

80. Kirane YM, Lewis GS, Sharkey NA, Armstrong AD. Mechanical characteristics of a novel posterior-step prosthesis for biconcave glenoid defects. J Shoulder Elb Surg. 2012;21(1):105–15.

81. Knowles NK, Ferreira LM, Athwal GS. The arthritic glenoid: anatomy and arthroplasty designs. Curr Rev Musculoskelet Med. 2016;9(1):23–9.

82. Smith MJ, Loftis CM, Skelley NW. Eccentric reaming for B2 glenoids: history, preoperative planning, surgical technique, and outcome. J Shoulder Elb Surg. 2019;3(1):1–8.

83. Ho JC, Amini MH, Entezari V, Jun BJ, Alolabi B, Ricchetti ET, Iannotti JP. Clinical and radiographic outcomes of a posteriorly augmented glenoid component in anatomic total shoulder arthroplasty for primary osteoarthritis with posterior glenoid bone loss. J Bone Joint Surg Am 2018;100(22):1934–1948.

84. Priddy M, Zarezadeh A, Farmer KW, Struk AM, King JJ, Wright TW, Schoch BS. Early results of augmented anatomic glenoid components. J Shoulder Elbow Surg 2019;28(6S):S138–S145.

85. Harmsen S, Casagrande D, Norris T. "Shaped" humeral head autograft reverse shoulder arthroplasty: treatment for primary glenohumeral osteoarthritis with significant posterior glenoid bone loss (B2, B3, and C type). Orthopade. 2017;46(12):1045–54.

86. Keener JD, Patterson BM, Orvets N, Aleem AW, Chamberlain AM. Optimizing reverse shoulder arthroplasty component position in the setting of advanced arthritis with posterior glenoid erosion: a computer-enhanced range of motion analysis. J Shoulder Elb Surg. 2018;27(2):339–49.

87. Friedman RJ, Barcel DA, Eichinger JK. Scapular notching in reverse total shoulder arthroplasty. J Am Acad Orthop Surg. 2019;27(6):200–9.

88. Berliner JL, Regalado-Magdos A, Ma CB, Feeley BT. Biomechanics of reverse total shoulder arthroplasty. J Shoulder Elb Surg. 2015;24(1):150–60.

89. Leathers MP, Ialenti MN, Feeley BT, Zhang AL, Ma CB. Do younger patients have better results after reverse total shoulder arthroplasty? J Shoulder Elb Surg. 2018;27(6S):24–8.

90. Vancolen SY, Elsawi R, Horner NS, Leroux T, Alolabi B, Khan M. Reverse total shoulder arthroplasty in the younger patient (≤65 years): a systematic review. J Shoulder Elb Surg. 2020;29(1):202–9.

91. Monir JG, Abeyewardene D, King JJ, Wright TW, Schoch BS. Reverse shoulder arthroplasty in patients younger than 65 years, minimum 5-year follow-up. J Shoulder Elb Surg. 2020:e1–7.